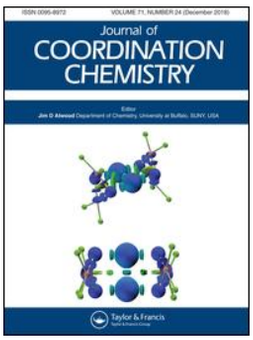

Journal of Coordination Chemistry

ISSN: 0095-8972 (Print) 1029-0389 (Online) Journal homepage: https://www.tandfonline.com/loi/gcoo20

Synthesis, characterization, crystal structure, and electrochemical properties of three copper(II) complexes with 3,5-dihalosalicylaldehyde Schiff bases derived from amantadine

Xu-Dong Jin, Han Wang, Xiao-Kang Xie, Jia-Yue Sun & He-Ming Liang

To cite this article: Xu-Dong Jin, Han Wang, Xiao-Kang Xie, Jia-Yue Sun & He-Ming Liang (2019): Synthesis, characterization, crystal structure, and electrochemical properties of three copper(II) complexes with 3,5-dihalosalicylaldehyde Schiff bases derived from amantadine, Journal of Coordination Chemistry, DOI: 10.1080/00958972.2019.1655643

To link to this article: https://doi.org/10.1080/00958972.2019.1655643

JOURNAL OF COORDINATION CHEMISTRY
https://doi.org/10.1080/00958972.2019.1655643

Synthesis, characterization, crystal structure, and electrochemical properties of three copper(II) complexes with 3,5-dihalosalicylaldehyde Schiff bases derived from amantadine

Xu-Dong Jin, Han Wang, Xiao-Kang Xie, Jia-Yue Sun and He-Ming Liang

College of Chemistry, Liaoning University, Shenyang, People's Republic of China

ABSTRACT

Complexes **1**-**3**, $C_{34}H_{36}X_4CuN_2O_2$ (X = Cl, Br, I), were synthesized with copper chloride dihydrate and three new Schiff base ligands derived from amantadine and 3,5-dihalosalicylaldehydes. They were characterized by IR, UV–VIS, elemental analysis, molar conductance, and single-crystal X-ray diffraction. Single-crystal X-ray diffraction analysis reveals that **1** and **2** crystallize in the triclinic system, $P\bar{1}$ space group. Each asymmetric unit consists of one copper(II) ion, two corresponding deprotonated Schiff base ligands and one lattice dichloromethane molecule. **3** crystallizes in the monoclinic system, $P2_1/n$ space group. Each asymmetric unit consists of one copper(II) ion and two deprotonated iodo-Schiff base ligands. The tetra-coordination of the central copper(II) ion in **1**-**3** is constructed by two nitrogen atoms and two oxygen atoms from the corresponding Schiff base ligands, forming a distorted tetrahedral geometry. Electrochemical properties of the complexes were determined by cyclic voltammetry.

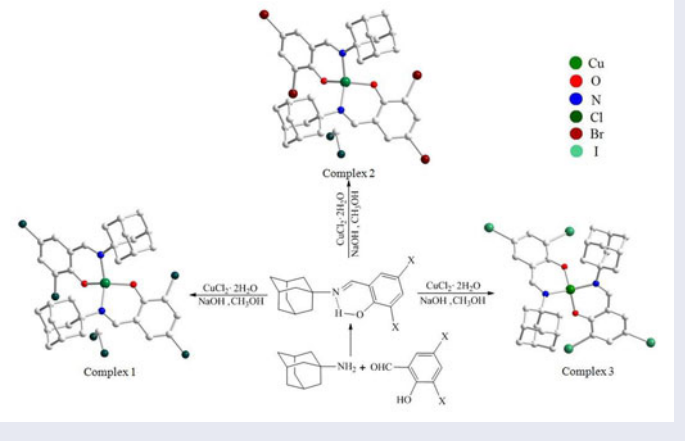

ARTICLE HISTORY
Received 2 April 2019
Revised 23 July 2019
Accepted 26 July 2019

KEYWORDS
Copper(II) complex; amantadine; 3,5-dihalosalicylaldehyde Schiff base; synthesis; crystal structure; electrochemical property

CONTACT Xu-Dong Jin 386237385@qq.com

Supplemental data for this article is available online at https://doi.org/10.1080/00958972.2019.1655643.

1. Introduction

Transition metal complexes with Schiff base ligands have been extensively investigated due to their biological activities, catalytic activities, electronic properties, and photochemical reactions [1–3] and are commonly used as antiviral, antitumor, and antibacterial agents [4, 5]. They can also be applied as electrode modifiers in electroanalysis [6–9]. Copper is one of the integral trace elements in human beings, playing a significant role in enzyme active sites [10, 11]. As a transition metal ion, copper(II) may have a wide range of coordination geometries [12]. Copper complexes with Schiff bases can be used to develop surface modified electrodes for sensor applications [13].

In many countries, amantadine (Symmetrel™) and rimantadine (Flumadine™) have been widely used to treat or prevent seasonal influenza as efficacious remedies [14–17]. It can also alleviate Parkinson symptoms [18, 19]. Salicylaldehyde and substituted salicylaldehydes, especially halogenated salicylaldehydes, were used to produce herbicides, insecticides and fungicides [20–22]. As an extension of our previous studies on the electrochemical properties of copper complexes with Schiff bases derived from amantadine or rimantadine [23, 24], we designed and synthesized three copper(II) complexes with the Schiff bases derived from amantadine and 3,5-dihalosalicylaldehydes.

The coordination behaviors of the ligands towards copper(II) were investigated and their absolute structures were determined by single-crystal X-ray diffraction analysis. Moreover, electrochemical properties of the complexes were determined by cyclic voltammetry in dimethylformamide (DMF) and dichloromethane.

2. Experimental

2.1. Materials and methods

All chemicals and solvents were purchased from Sinopharm Chemical Reagent. They were of analytical grade and used without purification. Elemental analyses were carried out on a Perkin Elmer Flash EA 1112. Infrared spectra (IR) were scanned from 4000 to 400 cm^{-1} via KBr pellets on a Nicolet NEXUS FT-IR 5700 spectrophotometer. UV–VIS spectra were measured on a Perkin Elmer Lambda 25 spectrophotometer. Melting points were measured on a WRS-1B micro melting point apparatus and are uncorrected. ^1H NMR chemical shifts (δ) for the Schiff base ligands were recorded at 300 MHz on a Varian Mercury-Vx300 spectrometer in $CDCl_3$ solvent containing TMS as an internal standard. The molar conductance for the complexes in DMF (1.0×10^{-3} mo1 L^{-1}) were measured using a DDS-11A conductometer.

2.2. Synthesis of the ligands

Three Schiff base ligands, 2-((adamantan-1-ylimino)methyl)-4,6-dichlorophenol (**HL^1**), 2-((adamantan-1-ylimino)methyl)-4,6-dibromophenol (**HL^2**) and 2-((adamantan-1ylimino)-methyl)-4,6-diiodophenol (**HL^3**), were prepared analogously to the literature [25, 26]. The general synthetic route for ligands in this work is shown in Figure 1.

Amantadine hydrochloride (563 mg, 3.0 mmol) and potassium hydroxide (168 mg, 3.0 mmol) in 50 mL anhydrous ethanol were stirred for 10 min and white precipitates

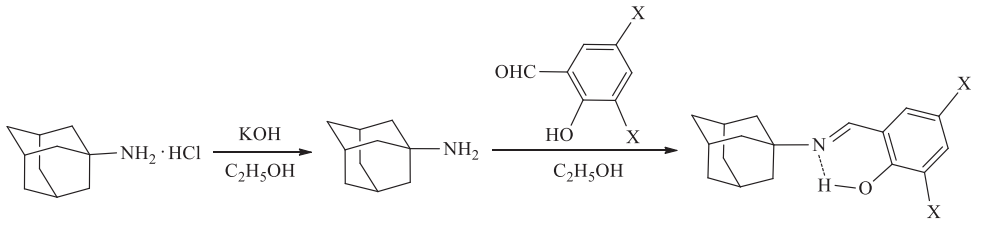

$\mathbf{HL^1}$: X = Cl; $\mathbf{HL^2}$: X = Br; $\mathbf{HL^3}$: X = I.

Figure 1. The formation of the Schiff base ligands.

(KCl) were filtered out. Then the transparent liquid was added dropwise to a solution of 3,5-dihalosalicylaldehydes (halo = Cl, Br, I; 382, 560, 748 mg; 2.0 mmol) in 30 mL anhydrous ethanol. The mixture was refluxed for 1 h and then cooled to room temperature. The yellow Schiff base precipitates were collected after 1 week of slow solvent evaporation.

$\mathbf{HL^1}$: 390 mg, yield 61%. Orange block. M.p. 167.5 ~ 168.5 °C. UV–VIS (dichloromethane, $c = 1 \times 10^{-5}$ g mL^{-1}): λ_{max} = 235 (0.9470), 333 (0.1174), 429 (0.1464); λ_{min} = 305 (0.0497), 369 (0.0481). ^{1}H NMR ($CDCl_3$, 300 MHz): δ 15.67 (*d*, $^3J = 4.2$, 1 H, Ar-OH); 8.12 (*d*, $^3J = 5.1$, 1 H, CH = N); 7.41 (*dd*, $^4J = 2.1/2.4$, 1 H, Ar-H); 7.09 (*d*, $^4J = 2.4$, 1 H, Ar-H); 2.22 (*s*, 3 H, CH, adam.H); 1.89 (*s*, 6 H, CH_2, adam.H); 1.80 - 1.67 (*m*, 6 H, CH_2, adam.H). *Anal*. Calc. for $C_{17}H_{19}Cl_2NO$ (324.24): C, 62.97; H, 5.91; N, 4.32. Found: C, 62.92; H, 5.86; N, 4.35.

$\mathbf{HL^2}$: 690 mg, yield 83%. Yellow powder. M.p. 175.7 ~ 176.5 °C. UV–VIS (dichloromethane, $c = 1 \times 10^{-5}$ g mL^{-1}): λ_{max} = 235 (1.2255), 339 (0.1289), 430 (0.2004); λ_{min} = 313 (0.0730), 371 (0.0573). ^{1}H NMR ($CDCl_3$, 300 MHz): δ 8.08 (*s*, 1 H); 7.70 (*d*, $^4J = 2.24$, 1 H); 7.29 (*d*, $^4J = 2.21$, 1 H); 2.22 (*s*, 3 H, CH); 1.90 (*s*, 6 H, CH_2); 1.67-1.81 (*m*, 6 H, CH_2). *Anal*. Calc. for $C_{17}H_{19}Br_2NO$ (413.15): C, 49.42; H, 4.64; N, 3.39. Found: C, 49.47; H, 4.61; N, 3.35.

$\mathbf{HL^3}$: 620 mg, yield 61%. Yellow floc. M.p. 178.5 ~ 179.5 °C. UV–VIS (dichloromethane, $c = 1 \times 10^{-5}$ g/mL): λ_{max} = 242 (1.1883), 346 (0.1094), 434 (0.2266); λ_{min} = 330 (0.1001), 403 (0.1379). ^{1}H NMR ($CDCl_3$, 300 MHz): δ 15.68 (*s*, 1 H, Ar-OH); 8.05 (*d*, $^4J = 2.1$, 1 H, Ar-H); 7.97 (*s*, 1 H, CH=N); 7.45 (*d*, $^4J = 2.1$, 1 H, Ar-H); 2.34 (*s*, 3 H, CH, adam.H); 1.90 (*d*, $J = 2.4$, 6 H, CH_2, adam.H); 1.80–1.67 (*m*, 6 H, CH_2, adam.H). *Anal*. Calc. for $C_{17}H_{19}I_2NO$(507.15): C, 40.26; H, 3.78; N, 2.76. Found: C, 40.34; H, 3.82; N, 2.73.

2.3. Synthesis of the complexes

Complexes bis(2-(1-adamantyliminomethyl)-4,6-dichlorophenolato-*N,O*)copper(II) (**1**), bis(2-(1-adamantyliminomethyl)-4.6-dibromophenolato-*N,O*)copper(II) (**2**) and bis(2-(1-adamantyliminomethyl)-4,6-diiodophenolato-*N,O*)copper(II) (**3**) were prepared in a similar procedure with a corresponding Schiff base ligand, NaOH, and copper(II) chloride dihydrate in anhydrous methanol, respectively (Figure 2).

NaOH (80 mg, 2.0 mmol) in 20 mL of anhydrous methanol was added to a stirring solution of a ligand ($\mathbf{HL^1}$, $\mathbf{HL^2}$, $\mathbf{HL^3}$; 648, 826, 1014 mg; 2.0 mmol) in 20 mL anhydrous methanol. The mixture was stirred for 20 min and then copper(II) chloride

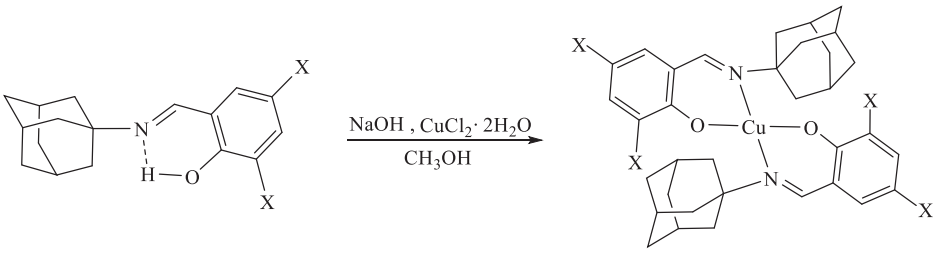

1: X = Cl; **2**: X = Br; **3**: X = I

Figure 2. Proposed structures of the complexes.

dihydrate (170 mg, 1.0 mmol) in 10 mL of anhydrous methanol was added dropwise. The mixed solution was refluxed for 2 h and then kept at room temperature until a large amount of precipitate was observed. The solid product was isolated by suction filtration, washed with a few drops of anhydrous methanol and dried.

1: 660 mg, yield 93%. Dark taupe powder. M.p. $>$ 300 °C. UV–VIS (dichloromethane, $c = 1.0 \times 10^{-5}$ g mL^{-1}): λ_{max} = 245 (0.9851), 327 (0.1674), 384 (0.2476); λ_{min} = 305 (0.1301), 348 (0.1411). *Anal*. Calc. for $C_{34}H_{36}Cl_4CuN_2O_2$ (710.02): C, 57.51; H, 5.11; N, 3.94. Found: C, 57.45; H, 5.15; N, 3.98.

2: 830 mg, yield 93%. Dark taupe powder. M.p. $>$ 300 °C. UV–VIS (dichloromethane, $c = 1.0 \times 10^{-5}$ g mL^{-1}): λ_{max} = 246 (0.9555), 330 (0.1609), 385 (0.2438); λ_{min} = 306 (0.1246), 348 (0.1401). *Anal*. Calc. for $C_{34}H_{36}Br_4CuN_2O_2$ (887.72): C, 46.01; H, 4.09; N, 3.16. Found: C, 46.04; H, 4.13; N, 3.12.

3: 980 mg, yield 91%. Taupe powder. M.p. $>$ 300 °C. UV–VIS (dichloromethane, $c = 1.0 \times 10^{-5}$ g mL^{-1}): λ_{max} = 246 (0.9670), 329 (0.1853), 389 (0.2348); λ_{min} = 354 (0.1530). *Anal*. Calc. for $C_{34}H_{36}I_4CuN_2O_2$ (1075.83): C, 37.96; H, 3.73; N, 2.60. Found: C, 37.93; H, 3.75; N, 2.62.

2.4. X-ray crystallography

Single crystals of **1**–**3** suitable for X-ray analysis were developed from a solution of CH_3OH/CH_2Cl_2 (1:2 v/v) through slow evaporation at room temperature. The crystallographic data collections were conducted on a Bruker Smart Apex II CCD with graphite monochromated Mo *K*α radiation ($\lambda = 0.71073$ Å) using the ω-scan technique. The data were integrated by using the SAINT program, which also corrected the intensities for Lorentz and polarization effects [27]. An empirical absorption correction was applied using SADABS [28]. The molecular structures were solved by SIR2004 [29] for **1** and SHELXS [30] for **2** and **3**. All non-hydrogen atoms were refined anisotropically on F^2 by the full-matrix least-squares technique using the SHELXL crystallographic software package [31]. Hydrogens were generated geometrically. All calculations were performed on a personal computer with the SHELXL crystallographic software package. Details of the crystal parameters, data collection, and refinement are summarized in Table 1. Selected bond lengths and angles with their estimated standard deviations are given in Table 2. The absolute structures for complexes, which were visualized by Diamond [32], are shown in Figures 3–5. The weak C–H···X and halogen bond interactions of **1**–**3** are shown in Figures 6–8.

Table 1. Crystallographic data for 1–3.

Empirical formula	$C_{34}H_{36}Cl_4CuN_2O_2{\cdot}CH_2Cl_2$ (**1**)	$C_{34}H_{36}Br_4CuN_2O_2{\cdot}CH_2Cl_2$ (**2**)	$C_{34}H_{36}I_4CuN_2O_2$ (**3**)
Formula weight (g mol^{-1})	794.91	972.75	1075.79
Crystal size (mm)	0.25 × 0.22 × 0.21	0.15 × 0.10 × 0.10	0.25 × 0.14 × 0.09
Crystal system	Triclinic	Triclinic	Monoclinic
Space group	$P\bar{1}$	$P\bar{1}$	$P2_1/n$
a (Å)	9.9535(6)	9.9860(4)	14.202(7)
b (Å)	11.8309(7)	11.9005(5)	9.972(5)
c (Å)	16.8277(10)	16.9848(7)	25.097(12)
α (°)	110.347(2)	109.9409(18)	90.00
β (°)	92.772(2)	92.801(2)	95.677(10)
γ (°)	110.812(2)	110.7636(19)	90.00
V (Å^3)	1703.00(18)	1740.78(13)	3537(3)
Z	2	2	4
θ range (°)	3.1 – 28.31	3.1 – 28.4	2.9 – 25.02
Index ranges	$-13 \leq h \leq 13$ $-15 \leq k \leq 15$, $-22 \leq l \leq 22$	$-13 \leq h \leq 13$ $-15 \leq k \leq 15$ $-22 \leq l \leq 22$	$-16 \leq h \leq 15$ $-11 \leq k \leq 11$ $-29 \leq l \leq 29$
ρ (g cm^{-3})	1.550	1.856	2.020
μ (mm^{-1})	1.148	5.407	4.141
Reflections collected / Unique	81637 / 8507 [R(int) = 0.0692]	89924 / 8683 [R(int) = 0.0486]	32970 / 6237 [R(int) = 0.1200]
Data / restraints / parameters	8507 / 0 / 415	8683 / 0 / 415	6237 / 6 / 388
Goodness-of-fit (GoF)	1.104	1.119	1.106
F(000)	818.0	962.0	2044.0
T/K	296(2)	223(2)	150(2)
R_1[a]/wR_2[b] ($I > 2\sigma(I)$)	0.0364 / 0.0927	0.0301 / 0.0692	0.0602 / 0.1257
R_1/wR_2 (all data)	0.0414 / 0.0973	0.0368 / 0.0721	0.1042 / 0.1407

[a] $R_1 = \Sigma||F_o|-|F_c||/|F_o|$.
[b] $wR_2 = [\Sigma w(F_o^2-F_c^2)^2/\Sigma w(F_o^2)^2]^{1/2}$

2.5. Electrochemical studies

The solvent, copper(II) chloride dihydrate, Schiff base ligands, and copper(II) complexes were investigated by cyclic voltammetry. They were prepared with a concentration of 1.0×10^{-3} mol L^{-1} in DMF and CH_2Cl_2, respectively. Electrochemical data were collected using a CHI 660E Electrochemical Workstation (Shanghai Chenhua). A three-electrode cell was used for all electrochemical experiments. This system consisted of glassy carbon (working), platinum wire (counter) and Ag/AgCl (reference) electrodes. Test solutions contained 1.0×10^{-3} mol compounds and 0.15 mol tetra-*n*-butylammonium hexafluorophosphate in DMF and CH_2Cl_2 solution. During the cyclic voltammetry measurement a constant flux of N_2 was kept over the solution surface in order to check the diffusion of atmospheric oxygen into the solution. All measurements were carried out at room temperature. The electroactivity range for this system was 3.0 V (from −1.5 to 1.5 V vs. SCE) at a scan rate of 100 mV s^{-1}. The data were integrated by using the OriginPro 8 program [33].

3. Results and discussion

3.1. Elemental analysis and molar conductance

Based on the elemental analysis, the C, H, N contents suggested that **1**–**3** consist of one copper(II) ion and two deprotonated ligands. Although all complexes are soluble in dichloromethane and chloroform, they are less soluble than their corresponding ligands in other solvents such as methanol, ethanol, acetone and dimethyl sulfoxide.

Table 2. Selected bond lengths (Å) and angles (°) for 1–3.

1		2		3	
Cu1-O1	1.8962(12)	Cu1-O1	1.8918(17)	Cu1-O1	1.906(7)
Cu1-N1	1.9993(14)	Cu1-N1	2.008(2)	Cu1-N1	2.001(8)
Cu1-O2	1.8917(13)	Cu1-O2	1.8952(17)	Cu1-O2	1.906(7)
Cu1-N2	2.0077(14)	Cu1-N2	1.998(2)	Cu1-N2	1.976(9)
N1-C7	1.283(2)	N1-C7	1.284(3)	N1-C7	1.284(13)
N1-C8	1.503(2)	N1-C8	1.500(3)	N1-C8	1.511(14)
N2-C24	1.289(2)	N2-C24	1.285(3)	N2-C24	1.282(13)
N2-C25	1.500(2)	N2-C25	1.503(3)	N2-C25	1.505(13)
O1-Cu1-O2	137.26(6)	O1-Cu1-O2	137.26(8)	O2-Cu1-O1	133.4(3)
O2-Cu1-N2	95.90(6)	O2-Cu1-N2	93.82(8)	O2-Cu1-N2	96.2(3)
O1-Cu1-N2	101.15(5)	O1-Cu1-N2	97.40(8)	O1-Cu1-N2	97.3(4)
O2-Cu1-N1	97.30(6)	O2-Cu1-N1	100.65(8)	O2-Cu1-N1	99.5(3)
O1-Cu1-N1	93.96(6)	O1-Cu1-N1	95.63(8)	O1-Cu1-N1	96.2(4)
N2-Cu1-N1	140.39(6)	N2-Cu1-N1	141.59(8)	N2-Cu1-N1	142.7(4)

The molar conductance values (Λ_M) are 4.1, 2.18 and 11.32 S cm^{-2} mol^{-1} for **1**–**3**, respectively, indicating that the complexes are non-electrolytic in nature [34].

3.2. IR spectra

IR spectra of the ligands and the complexes are provided in the Supplementary Material and the main IR data are collected in Table 3. In general, free O–H stretching vibration bands should be at 3500–3600 cm^{-1}, however, they display red-shifted values for **HL^1**-**HL^3** at 3440, 3416 and 3411 cm^{-1} due mainly to an effect of intramolecular hydrogen bonding. These vibrations are absent in the complexes, illustrating that phenolic OH groups are deprotonated as O → Cu coordination occurs. The strongest absorptions for the ligands at 1628, 1626 and 1627 cm^{-1} are assigned to the C=N stretch, which red-shifted to 1609, 1607 and 1610 cm^{-1} in **1**–**3**. In the complexes, these vibration bands undergo downward shift by 19, 19 and 17 cm^{-1}, implying coordination of the azomethine nitrogen atom to copper(II) [35, 36]. Bands at 1450–1475 cm^{-1} for ligands and 1431–1449 cm^{-1} for complexes are assigned to C–N stretching vibrations. Meanwhile, bands at 1213, 1212 and 1225 cm^{-1} for the ligands as well as 1169, 1154 and 1147 cm^{-1} for the complexes are C–O stretching vibrations [35]. In low frequency regions, the remarkable appearance of absorptions at 555–558 and 446–452 cm^{-1} for the complexes can be assigned to Cu–O and Cu–N vibrations, which indicate that oxygen and nitrogen atoms of the Schiff bases are coordinated to copper(II) [35, 36].

3.3. UV–VIS spectra

UV–VIS spectra of the ligands and the complexes are provided in the Supplementary Material. All the complexes show significant changes compared to their corresponding ligands from 200–600 nm. The absorption bands at 235–242 nm for the ligands and 245–246 nm for the complexes are clearly assigned to the π-π* transition of C=N and benzenoid conjugated systems. Bands at 333–346 nm for the ligands should be assigned to the π-π* transitions of the benzene ring, which were greatly influenced by the substituent groups. The corresponding complexes' absorptions are at 327–330 nm. Bands at 429 nm, 430 nm and 434 nm for **HL^1**-**HL^3** are attributed to n-π* transition of the C=N group. Besides the above, **1**–**3** have obvious absorption bands at 384, 385,

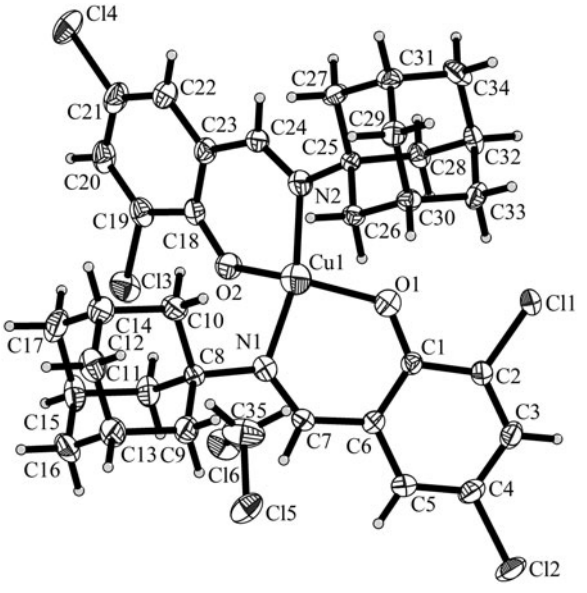

Figure 3. The molecular structure of **1**. Thermal ellipsoids are drawn at 50% of probability.

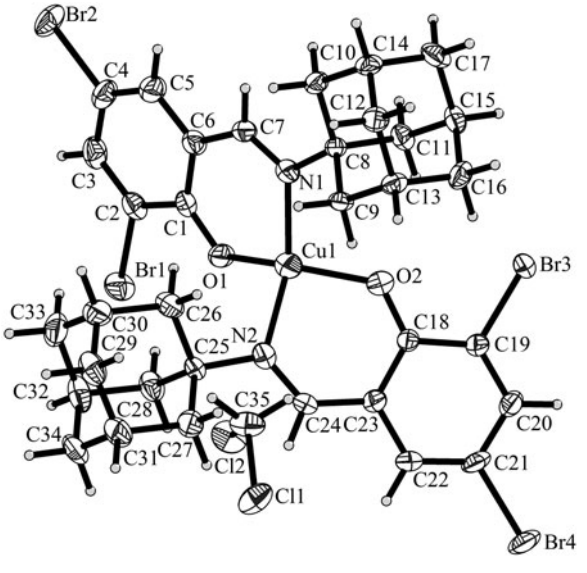

Figure 4. The molecular structure of **2**. Thermal ellipsoids are drawn at 50% of probability.

and 389 nm, respectively, which are assigned to charge transfer transitions from the ligands to copper(II) of N → Cu and O → Cu.

3.4. Crystal structures of complexes

The crystallographic analysis reveals that **1** and **2** crystallize in the triclinic system, $P\bar{1}$ space group; each asymmetric unit comprises one mononuclear complex molecule and one lattice dichloromethane molecule. Complex **3** crystallizes in the monoclinic

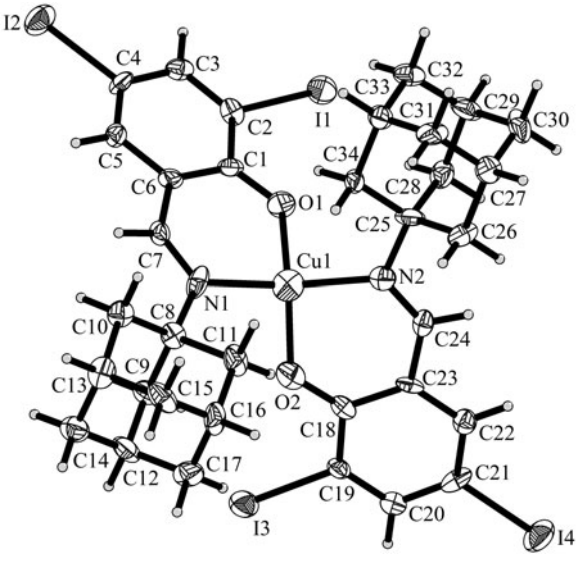

Figure 5. The molecular structure of **3**. Thermal ellipsoids are drawn at 50% of probability.

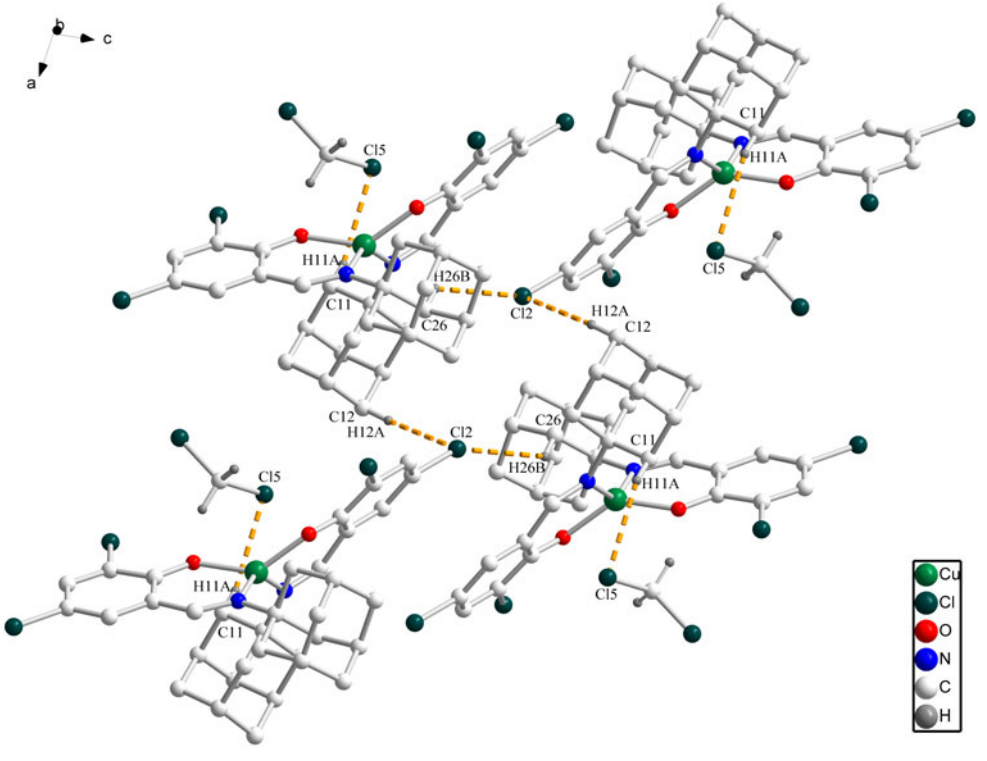

Figure 6. The short C-H···Cl contacts in the packing of **1**. View toward plane for hkl = 2.25, −11.68.

system, $P2_1/n$ space group; each asymmetric unit comprises one mononuclear complex molecule. The central copper(II) ion in **1**–**3** is bonded to the oxygen and nitrogen

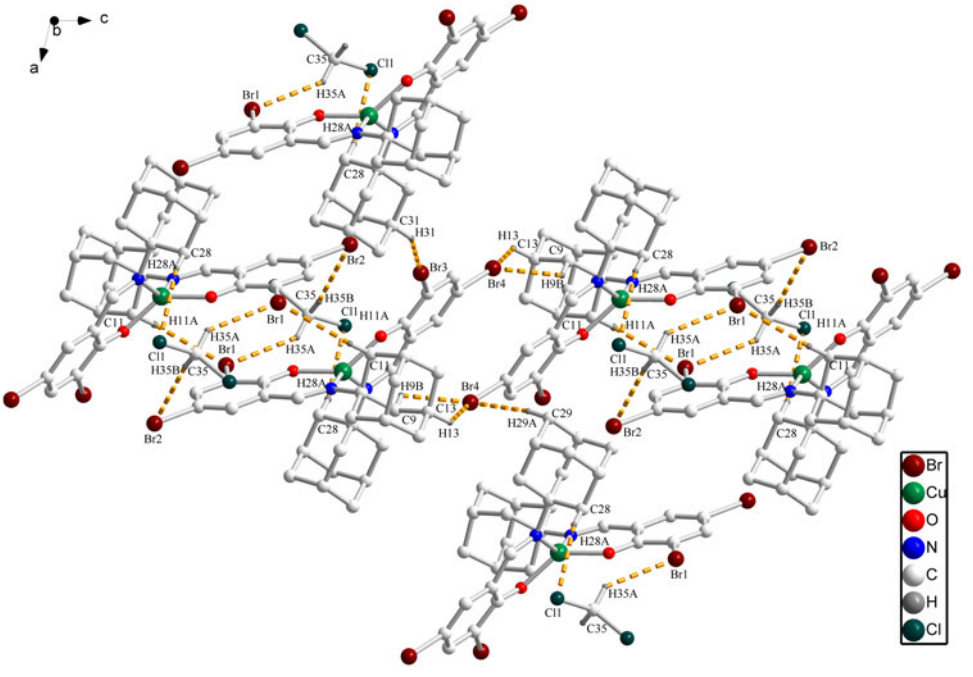

Figure 7. The short C-H···Cl and C-H···Br contacts in the packing of **2**. View toward plane for hkl = 3.38, −11.83.

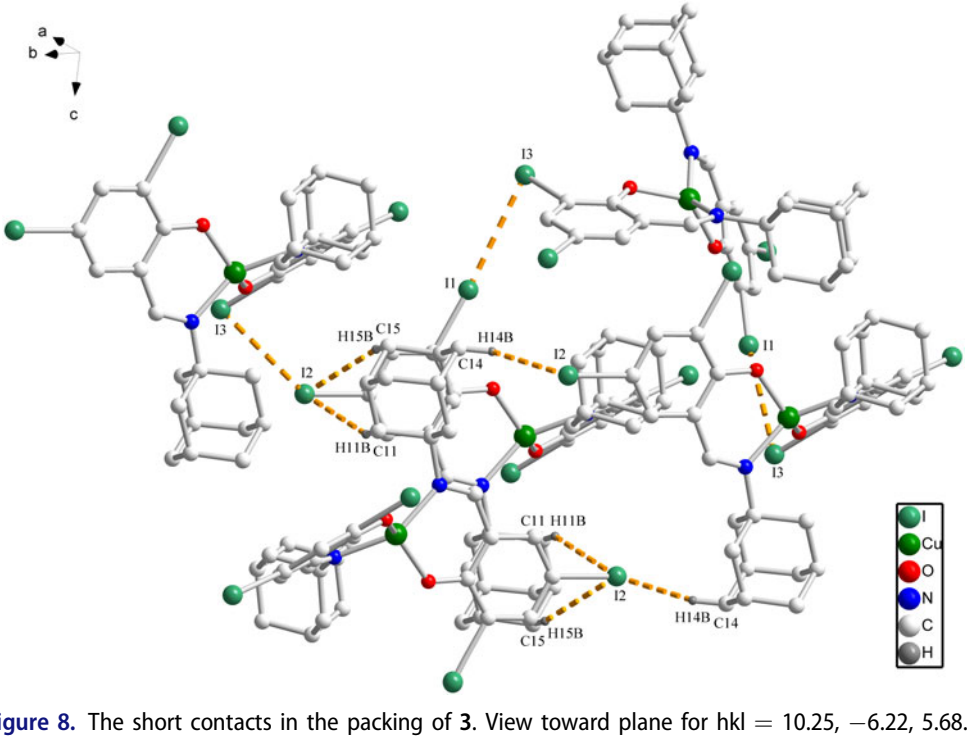

Figure 8. The short contacts in the packing of **3**. View toward plane for hkl = 10.25, −6.22, 5.68.

Table 3. Main IR data for HL^1-HL^3 and 1–3 (cm^{-1}).

Compound	υ_{O-H}	υ_{CH2}	$\upsilon_{C=N}$	υ_{C-N}	υ_{C-O}	υ_{M-O}	υ_{M-N}
HL^1	3440(w)	2849(s)	1628(s)	1458(s)	1213(s)	–	–
1	–	2850(m)	1610(s)	1449(s)	1168(s)	558(w)	452(w)
HL^2	3433(w)	2847(m)	1626(s)	1450(s)	1211(m)	–	–
2	–	2849(m)	1608(s)	1440(s)	1154(m)	556(w)	446(w)
HL^3	3411(w)	2850(m)	1627(s)	1475(m)	1225(m)	–	–
3	–	2848(w)	1610(s)	1431(s)	1147(m)	555(w)	451(w)

donors of the two bidentate Schiff base ligands. The dihedral angle between the two coordination planes of **1**–**3** defined by O1-Cu1-N1 and O2-Cu1-N2 is 56.95° for **1**, by O1-Cu1-N1 and O2-Cu1-N2 is 56.25° for **2**, and by O1-Cu1-N1 and O2-Cu1-N2 is 57.77° for **3**. The two phenyl rings are in the intersecting planes with a dihedral angle defined by C1-C3-C6 and C18-C20-C22 of 55.02° for **1**, by C6-C1-C2 and C18-C23-C22 of 54.71° for **2**, and by C2-C1-C6 and C18-C23-C22 of 66.89° for **3**. Moreover, bond angles also reveal that the coordination geometry of copper in **1**–**3** is distorted tetrahedral; the parameters $\tau_4 = [360-(\alpha+\beta)]/141°$ [37] for **1**–**3** are 0.58, 0.59 and 0.59, respectively, of which the angles are N2-Cu1-N1 (α) and O2-Cu1-O1 (β) (see Table 2). Complexes **1**–**3** are expected for typical Schiff base ligands (containing a short C=N bond distance of 1.283(2)/1.289(2) Å for **1**, 1.284(3)/1.285(3) Å for **2** and 1.282(13)/1.284(13) Å for **3**) coordinated to a metal center, where the imine form is predominant. The distinctly shortened Cu1-O1 and elongated Cu1-N1 bonds are 1.896(12) and 1.999(14) Å for **1**, 1.892(17) and 2.008(2) Å for **2**, and 1.906(7) and 2.001(8) Å for **3** (normal bond lengths are ca. 1.940 and 1.960 Å). Compared to similar CuN_2O_2 structures, it can be found that the C=N, Cu–O and Cu–N bond lengths are very close to those of compounds reported [23, 24], although they have different substituent groups on the benzene ring. However, the angles for the coordination geometry of central copper ion are distinct. For example, the geometry around copper(II) is distorted square planar with a small dihedral angle between the two coordination planes in salicylaldehyde and 4-methoxyl-salicylaldehyde Schiff bases copper(II) complexes. Another coincident case was found in 3-methoxy-salicylaldehyde Schiff bases copper(II) complex with the dihedral angle of 0°. In addition, the coordination geometry and the τ_4 parameter value of dihalogenated complexes **1**-**3** are very similar to the copper(II) complexes derived from mono-halogenated salicylaldehyde Schiff bases. The coordination geometry around the copper(II) ion reflects the Jahn-Teller effect [38]. The shortest distance between two adamantine carbons from two ligands is 4.129 Å for C10-C26 in **1**, 4.175 Å for C9-C26 in **2**, and 4.402 Å for C11-C34 in **3**, respectively. The distance of two neighboring copper ions along the y axis is 9.953 Å in **1**, 7.124 Å in **2**, and 8.631 Å in **3**. The bidentate coordination mode of **1**–**3** does not form intramolecular hydrogen bonds for the deprotonated ligands, but there still exist two six-membered rings through a copper(II), two oxygen and two nitrogen atoms [39].

The Mercury software has been used for obtaining the packing mode and data of intermolecular interactions. Though the angles of **1**–**3** between the two adjacent benzene rings in the stacking complexes are 1.85°, 0° and 0.87°, <10°, the distance between the centroid of benzene ring to the plane of another benzene ring is 6.721, 3.569 and 4.345 Å, >3.5 Å [40]. Thus, we can conclude that **1**–**3** do not possess π–π

stacking interactions. Complexes **1**–**3** are not found to possess weak C–H···π interactions, but rather several weak C–H···X (X = Cl, Br, I) interactions (Figures 6–8). Complex **1** has three C–H···Cl interactions, which can be distinguished as two situations. The first is about C11–H11A···Cl5 between the complex molecule and dichloromethane molecule in the asymmetric unit. The distance of C11···Cl5 is 3.776 Å. In another situation, C12–H12A···Cl2 and C26–H26B···Cl2 are observed, with distances of 3.828 and 3.550 Å, between adjacent complex molecules. Complex **2** has one weak C–H···Cl interaction and seven weak C–H···Br interactions. They are summarized also in two situations, one in which C28–H28A···Cl1, C35–H35A···Br1 and C35–H35B···Br2 are formed through the complex molecule and a dichloromethane molecule. The distances of C···X are 3.803, 3.820 and 3.902 Å, respectively. The other five weak C–H···Br interactions (C11–H11A···Br1, C31–H31···Br3, C9–H9B···Br4, C13–H13···Br4, and C29–H29A···Br4) are formed between adjacent copper complex molecules. The C···Br distances are 3.824, 3.702, 3.584, 3.621 and 3.902 Å in turn. Complex **3** possesses three weak interactions. C11–H11B···I2, C15–H15B···I2 and C14–H14B···I2 are formed from adjacent complex molecules. The C···I distances are 4.028, 4.006 and 3.866 Å, respectively.

Complexes **1** and **2** are not found to possess halogen bonding interactions, but **3** possesses two kinds of weak intermolecular I···I interactions in the packing structure. Both I1···I3 and I2···I3 interactions are formed through adjacent copper complex molecules. I1···I3 interaction belongs to the type II motifs with the characteristic of θ_1 86.57° and θ_2 172.89°, respectively, where θ_1 and θ_2 are the C-I···I angles [41]. The I1···I3 distance is 3.79 Å close to the D_{anis} value 3.89 Å for type II. The I2···I3 distance is 3.95 Å and the value of θ_1 and θ_2 are 89.29° and 139.52°, respectively. The weak C–H···X interactions and halogen bonds help stabilize the crystal structure and form an infinitive three-dimensional structure.

3.5. Electrochemistry

The electrochemical behavior was investigated in DMF and dichloromethane containing tetra-*n*-butylammonium hexafluorophosphate as a supporting electrolyte. As shown in Figure 9(a), the solvent was tested under the addition of 0.15 mol supporting electrolyte; no redox peak was found in the scanning region. In Figure 9(b), copper chloride dihydrate exhibited a quasi-reversible oxidation and reduction peak at 0.343 ($\boldsymbol{E}_{pc}$) and 0.473 V vs. Ag/AgCl ($\boldsymbol{E}_{pa}$) in DMF solution. The $\Delta\boldsymbol{E}_p = (\boldsymbol{E}_{pa} - \boldsymbol{E}_{pc})$ value is 130 mV and the i_{pa}/i_{pc} ratio is 1.107. At the potentials of 0.850 ($\boldsymbol{E}_{pc}$) and 1.200 V vs. Ag/AgCl ($\boldsymbol{E}_{pa}$) also exists a redox peak. Because copper chloride dihydrate is insoluble in dichloromethane, its electrochemical behaviors in dichloromethane are not available.

The cyclic voltammograms of the ligands are shown in Figures 10 and 11. In DMF solution, $\mathbf{HL^1}$-$\mathbf{HL^3}$ exhibit very similar oxidation peaks at 1.151, 1.159 and 1.130 V vs. Ag/AgCl; the corresponding reduction peaks are not observed. In dichloromethane solution, in anodic potential regions, $\mathbf{HL^1}$-$\mathbf{HL^3}$ exhibit oxidation peaks at 1.350, 1.372 and 1.347 V vs. Ag/AgCl, respectively. $\mathbf{HL^2}$ and $\mathbf{HL^3}$ have the reverse weak reduction peaks at 1.135 and 1.102 V vs. Ag/AgCl, but the peaks are not observed for $\mathbf{HL^1}$. In the

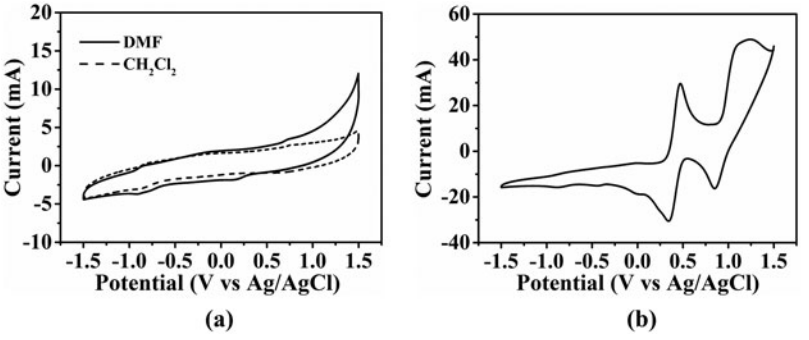

Figure 9. The cyclic voltammogram for solvent (a) and $CuCl_2{\cdot}2H_2O$ (b) in DMF solution.

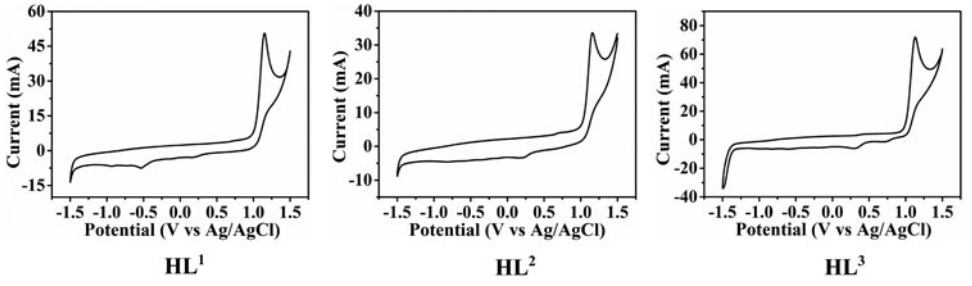

Figure 10. The cyclic voltammogram for **HL**^{1}-**HL**^{3} in DMF solution.

cathodic potential region, **HL**^{1}-**HL**^{3} exhibit reduction peaks at −0.794, −0.777 and −0.769 V vs. Ag/AgCl, which can be assigned to the reduction of the imine group [42].

The cyclic voltammograms of the complexes are shown in Figures 12 and 13. The data for the complexes are collected in Table 4. Compared with the cyclic voltammogram of the solvent, copper chloride dihydrate and ligands, all complexes perform reversible reductive responses in cathodic potential regions. In DMF solution, the reduction potentials for **1**–**3** are observed at −0.765, −0.750 and −0.752 V vs. Ag/AgCl ($\boldsymbol{E}_{pc}$), respectively, the characteristic peak B for Cu(II) → Cu(I). The corresponding $\boldsymbol{E}_{pa}$ values are observed at -0.688, -0.671 and -0.674 V vs. Ag/AgCl, the peak A for Cu(I) → Cu(II). The $\Delta\boldsymbol{E}_p = (\boldsymbol{E}_{pa} - \boldsymbol{E}_{pc})$ values of **1**–**3** are 77, 80 and 78 mV, respectively. Furthermore, the i_{pa}/i_{pc} ratios are 0.92, 0.83 and 0.81, respectively. These results indicate the quasi-reversibility character of the redox process.

DMF is a commonly used solvent for measuring electrochemical properties, but it is a highly coordinating solvent that the Cu center might be interacting with in a non-negligible manner. Therefore, the tests were also carried out in dichloromethane. There have exhibited similar oxidation and reduction potential peaks at $E_{1/2}$ −0.454, −0.434, and −0.459 V vs. Ag/AgCl in dichloromethane solution. Peak D is characteristic of the Cu(II) → Cu(I) couple, while C is assigned to Cu(I) → Cu(II) couple. The peak potential is shifted to more positive potential compared to that in DMF. Furthermore, the midpoint potentials of **1**−**3** are very similar in both DMF and dichloromethane, which indicate that the halogen substituent has no obvious effect on the electrochemical behavior. This conclusion is different from previous literature [24]. The $\Delta\boldsymbol{E}_p$ value and i_{pa}/i_{pc} ratios of the complexes reveal that the redox process is quasi-reversible in

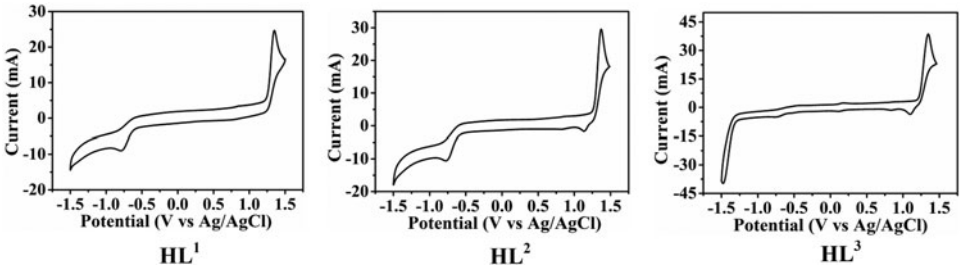

Figure 11. The cyclic voltammogram for **HL**[1]-**HL**[3] in dichloromethane solution.

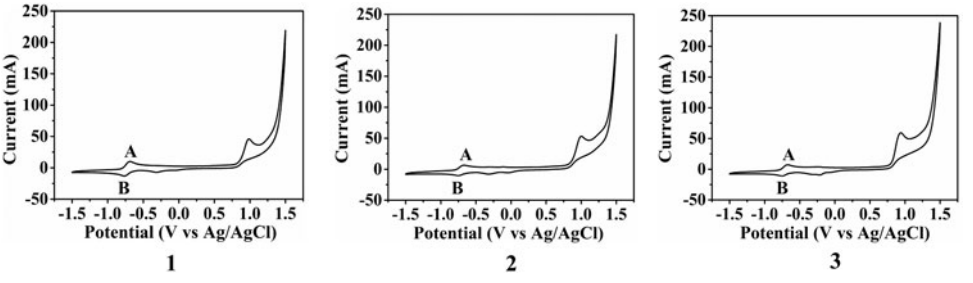

Figure 12. The cyclic voltammogram for **1**–**3** in DMF solution.

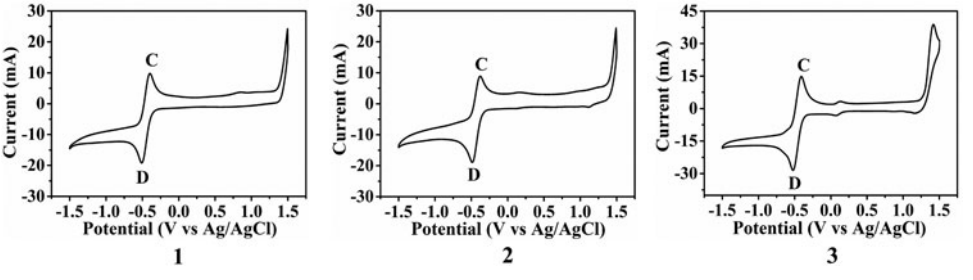

Figure 13. The cyclic voltammogram for **1**–**3** in dichloromethane solution.

Table 4. Redox potential data of 1–3 in DMF and dichloromethane solution.

Compound	Solvent	E_{pa}/V	E_{pc}/V	ΔE_p/mV	$E_{1/2}$/V	i_{pa}/i_{pc}
1	DMF	−0.688	−0.765	77	−0.727	0.92
	Dichloromethane	−0.397	−0.510	113	−0.454	0.93
2	DMF	−0.671	−0.750	80	−0.711	0.83
	Dichloromethane	−0.380	−0.488	108	−0.434	0.77
3	DMF	−0.674	−0.752	78	−0.713	0.81
	Dichloromethane	−0.402	−0.515	113	−0.459	0.97

dichloromethane. For copper(II) complexes with Schiff base ligands, a peak current ratio less than unity [43] can be commonly observed [44, 45]. This behavior can be attributed to the existence of trace water in the solvent or supporting electrolyte according to the literature [46]. In addition, it is reported that the $Cu(II)L_2/[Cu(I)L_2]$ reaction in most CuN_2O_2 coordination complexes is quasi-reversible because the $[Cu(I)L_2]$ species are chemically decomposed to a copper ion, which is subsequently is reduced to copper metal [47].

4. Conclusion

Three Schiff base ligands and their corresponding copper(II) complexes have been prepared and their structures were characterized. Single-crystal X-ray diffraction analyses revealed that each complex molecule consists of one copper(II) ion and two deprotonated Schiff base ligands. The Schiff base ligands serve as bidentate ligands coordinating through an oxygen atom and a nitrogen atom to the copper(II) ion. The geometry around the metal in the complexes is distorted tetrahedral. The electrochemical properties of the complexes revealed the quasi-reversible one electron transfer redox processes.

Funding

This work was financially supported by Foundation of Liaoning Provincial Department of Education Innovation Team Projects (grant number LT2017010); the Cause of Public Welfare Scientific Research Fund (grant number 2015005008); Shenyang Science and Technology Plan Project (grant number F13-289-1-00); Liaoning University's College Students Innovation and Entrepreneurship Training Program (grant number x201610140158).

References

[1] N.K. Dutt, K. Nag. *J. Inorg. Nulc. Chem.*, **30**, 2493 (1968).
[2] R.D. Campo, J.J. Criado, E. García, M.R. Hermosa, A. Jiménez-Sánchez, J.L. Manzano, E. Monte, E. Rodríguez-Fernández, F. Sanz. *J. Inorg. Biochem.*, **89**, 74 (2002).
[3] Z.H. Chohan, H. Pervez, A. Rauf, A. Scozzafava, C.T. Supuran. *J. Enzyme Inhib. Med. Chem.*, **17**, 117 (2002).
[4] A. Jarrahpour, D. Khalili, E.D. Clercq, C. Salmi, J.M. Brunel. *Molecules*, **12**, 1720 (2007).
[5] R. Katwal, H. Kaur, G. Sharma, M. Naushad, D. Pathania. *J. Ind. Eng. Chem.*, **31**, 173 (2015).
[6] D.M. Boghaei, A. Bezaatpour, M. Behzad. *J. Mol. Catal. A Chem.*, **245**, 12 (2006).
[7] T. Akitsu, Y. Einaga. *Polyhedron*, **24**, 1869 (2005).
[8] A.M. Elseman, D.A. Rayan, M.M. Rashad. *J. Mater. Sci: Mater. Electron.*, **27**, 2652 (2016).
[9] M.B. Gholivand, P. Niroomandi, A. Yari, M. Joshagani. *Anal. Chim. Acta*, **538**, 225 (2005).
[10] D.I. Arnon. *Plant Physiol.*, **24**, 1 (1949).
[11] G. Grass, C. Rensing, M. Solioz. *Appl. Environ. Microbiol.*, **77**, 1541 (2011).
[12] B.J. Hathaway. *Struct. Bonding (Berlin)*, **57**, 55 (1984).
[13] L. Mao, K. Yamamoto, W. Zhou, L. Jin. *Electroanalysis*, **12**, 72 (2000).
[14] A. Tsunoda, H.F. Maassab, K.W. Cochran, W.C. Eveland. *Antimicrob. Agents Chemother. (Bethesda)*, **5**, 553 (1965).
[15] F.G. Hayden, A. Minocha, D.A. Spyker, H.E. Hoffman. *Antimicrob. Agents Chemother.*, **28**, 216 (1985).
[16] C. Schroeder, H. Heider, E. Möncke-Buchner, T. Lin. *Eur. Biophys. J.*, **34**, 52 (2005).
[17] R.M. Pielak, J.J. Chou. *Protein Cell.*, **1**, 246 (2010).
[18] M. Brenner, A. Haass, P. Jacobi, K. Schimrigk. *J. Neurol.*, **236**, 153 (1989).
[19] N. Nishikawa, M. Nagai, T. Moritoyo, H. Yabe, M. Nomoto. *Parkinsonism. Relat. D*, **15**, 351 (2009).
[20] L.C. Felton, J.H. Brewer. *Science*, **105**, 409 (1947).
[21] E.M. Hodnett, W.J. Dunn. *J. Med. Chem.*, **13**, 768 (1970).
[22] L. Shi, H.M. Ge, S.H. Tan, H.Q. Li, Y.C. Song, H.L. Zhu, R.X. Tan. *Eur. J. Med. Chem.*, **42**, 558 (2007).
[23] X.D. Jin, L. Kou, H.M. Liang, J. Tong, P. Zhang, G.C. Han, K.J. Ren, X.B. Zhao. *J. Coord. Chem.*, **69**, 3309 (2016).

[24] X.D. Jin, W.C. Wang, X.X. Feng, L.C. Bu, J. Tong, P. Zhang, K.J. Ren, X.B. Zhao. *Russ. J. Coord. Chem.*, **43**, 787 (2017).
[25] X.D. Jin, C. Xu, X.C. Liu, X.Y. Yin, Y.C. Gang, Q. Yang, Y.H. Jin. *J. Coord. Chem.*, **66**, 3970 (2013).
[26] C. Xu, X.C. Liu, X.D. Jin, Q. Yang, G.C. Han, Y.C. Gang, H.H. Hu. *J. Coord. Chem.*, **67**, 352 (2014).
[27] Bruker. *SAINT. Version 6.02a*, Bruker AXS, Madison, WI (2002).
[28] G.M. Sheldrick. *SADABS: Program for Bruker Area Detector Absorption Correction*, University of Göttingen, Germany (1997).
[29] M.C. Burla, R. Caliandro, M. Camalli, B. Carrozzini, G.L. Cascarano, L. De Caro, C. Giacovazzo, G. Polidori, D. Siliqi, R. Spagna. *J. Appl. Crystallogr.*, **40**, 609 (2007).
[30] G.M. Sheldrick. *Acta Crystallogr., A, Found. Crystallogr*, **64**, 112 (2008).
[31] G.M. Sheldrick. *Acta Crystallogr. C Struct. Chem.*, **C71**, 3 (2015).
[32] K. Brandenburg. *Diamond (Version 3.2 g)*, Crystal Impact GbR: Bonn, Germany (2011).
[33] C.Y. Gao, J.G. Niu, Q.C. Gao. *Appl. Mech. Mater.*, **580**, 509 (2014).
[34] S. Chandra, U. Kumar. *Spectrochim. Acta A Mol. Biomol. Spectrosc.*, **60**, 2825 (2004).
[35] R.C. Felicio, G.A. da Silva, L.F. Ceridorio, E.R. Dockal. *Synth. React. Inorg. Met. Org. Chem.*, **29**, 171 (1999).
[36] G.C. Percy, D.A. Thornton. *J. Inorg. Nucl. Chem.*, **35**, 2319 (1973).
[37] L. Yang, D.R. Powell, R.P. Houser. *Dalton Trans.*, **9**, 955 (2007).
[38] X.L. Zhang. *Chin. J. Struct. Chem.*, **32**, 236 (2013).
[39] M. Zeller, A.D. Hunter. *Acta Crystallogr. E Struct. Rep. Online*, **E61**, m23 (2005).
[40] M.L. Główka, D. Martynowski, K. Kozłowska. *J. Mol. Struct.*, **474**, 81 (1999).
[41] P. Metrangolo, G. Resnati. *Halogen Bonding*, Springer-Verlag, Berlin (2008).
[42] V.T. Kasumov, A.I. Özturk, F. Köksal. *Polyhedron*, **26**, 3129 (2007).
[43] J. Heinze. *Angew. Chem. Int. Ed. Engl.*, **23**, 831 (1984).
[44] J.M. Fernández-G, E. Acevedo-Arauz, R. Cetina-Rosado, R.A. Toscano. *Trans. Met. Chem.*, **24**, 18 (1999).
[45] J.M. Fernández-G, M.D.R. Patiño-Maya, R.A. Toscano, L. Velasco, M. Otero-López, M. Aguilar-Martínez. *Polyhedron*, **16**, 4371 (1997).
[46] M.J. Samide, D.G. Peters. *J. Electroanal. Chem.*, **443**, 95 (1998).
[47] M. Aguilar-Martínez, R. Saloma-Aguilar, N. Macías-Ruvalcaba, R. Cetina- Rosado, A. Navarrete-Vázquez, V. Gómez-Vidales, A. Zentella-Dehesa, R.A. Toscano, S. Hernández-Ortega, J.M. Fernández-G. *J. Chem. Soc. Dalton Trans.*, **632**, 2346 (2001).